J. Cosmet. Sci., 68, 25–33 (January/February 2017)

Effect of SIRT6 knockdown on NF-κB induction and on residual DNA damage in cultured human skin fibroblasts

E. C. GOYARTS, K. DONG, E. PELLE, and N. PERNODET, *Estee Lauder Research Laboratories, Melville, NY (E.C.G., K. D., E. P., N. P.) and Environmental Medicine, New York University School of Medicine, New York, NY (E.P.).*

Accepted for publication October 24, 2016.

Synopsis

SIRT6 is a member of the sirtuin family, which is involved in multiple cellular pathways related to aging, inflammation, epigenetics, and a variety of other cellular functions, including DNA repair (1). Multiple pathways involving different cellular functions are impacted by the deacetylase activity of SIRT6. Genomic integrity is maintained by the capacity of SIRT6 to modulate the accessibility of DNA repair proteins. Glucose metabolism is suppressed by SIRT6 via the deacetylation of histones located at the promoter regions of multiple glycolytic genes and the corepression of hypoxia-inducible factor-1α. SIRT6 is also a corepressor of nuclear factor (NF)-κB, silencing NF-κB target genes through the deacetylation of histones at their promoters' regions. We used SIRT6 small-interfering RNA as a tool to modulate residual DNA damage and NF-κB expression in human dermal fibroblasts. We measured NF-κB levels in the presence or the absence of ultraviolet B (UVB). The impact of SIRT6 knockdown as shown by a decrease in SIRT6 messenger RNA levels resulted in residual DNA damage as evaluated by the comet assay. Our results show that NF-κB was increased significantly (up to 400%) due to SIRT6 silencing in the absence of UVB, illustrating the master regulatory function of SIRT6 in inflammation. We also found a significant increase in DNA damage without UV exposure as a result of SIRT6 silencing, indicating the importance of SIRT6 in DNA repair pathways in cultured human dermal fibroblasts.

INTRODUCTION

Sirtuins are a family of NAD^+-dependent histone deacetylases impacting a broad range of cellular functions (1,2). Mammals have seven sirtuins (SIRT1–7), which modulate diverse cellular functions including metabolism, cellular stress response, genomic stability, inflammation, and aging (3,4). SIRT6, which is localized in the nucleus, catalyzes the removal of an acetyl group at lysine 9 (H3K9) and/or lysine 56 (H3K56) of histone 3. Deacetylation of histone 3 reduces the accessibility of DNA-binding proteins because the nucleosomal structure becomes compressed. Thus, SIRT6 modulates many genes through posttranslational modification of histone 3 resulting in chromatin silencing (5). SIRT6 is considered

Address all correspondence to Earl C. Goyarts at egoyarts@estee.com.

to have strong antiaging benefits as SIRT6-deficient mice develop a progeroid-like syndrome resembling premature aging and die after 4 weeks (6).

Mammalian cells deficient in SIRT6 have defects in DNA repair resulting in genomic instability. These include base excision repair (BER) (6,7,8), double strand break (DSB) repair (7,9–12), and telomere maintenance (7,13,14). Current evidence indicates that SIRT6 regulates BER either by modulating BER factors or by regulating the chromatin density permitting the accessibility of BER factors to DNA damage sites (7,13). Successful DSB repair requires that SIRT6 recruit a chromatin remodeler, SNF2H, to the DSB (11) and the deacetylation of a C-terminal binding protein, CtIP, to promote DNA-end resectioning (10). Proper telomere maintenance requires the binding of SIRT6 to telomeric chromatin resulting in the deacetylation of H3K9 histones and preventing chromosome end fusion. Thus, SIRT6 functions both as an enzyme and as a scaffold for establishing a unique microenvironment for recruiting other proteins needed for DNA repair.

In addition to DNA repair, SIRT6 is involved in inflammation control (3). Pyrimidine dimers are the primary trigger of post-ultraviolet (UV) erythema and their removal requires DNA nicking in order to mediate excision repair (15). SIRT6 promotes tumor necrosis factor (TNF)-α secretion by deacylating two myristoyl groups from lysine residues at peptide positions 19 and 20 of TNF-α (16). Conversely, SIRT6 is recruited to promoter regions of nuclear factor (NF)-κB target genes and physically docks with the NF-κB subunit, RelA (5,17). SIRT6 silences these NF-κB target genes by modifying the chromatin via deacetylation of H3K9 on nearby histones (5,17). The altered chromatin structure destabilizes RelA binding to the target gene promoter, terminating NF-κB stimulation of the target genes. A SIRT6-deficient mouse survives only 30 days because both NF-κB genes are unregulated leading to hyperactive NF-kB signaling (18). A SIRT6-deficient mouse crossed with a *RelA* +/− mouse rescues early lethality of SIRT6-deficient mice, giving rise to progeny which survive for more than 100 days, indicating that a reduction of the NF-κB copy number results in longer survival (17,18). Further, recall that transgenic male mice overexpressing SIRT6 have increased longevity, about 15% (19), which is associated with the insulin-like growth factor 1 signaling pathway (3).

As mentioned earlier, a reduced capacity to maintain genomic integrity and an increased sensitivity to oxidative stress and inflammation are causes of premature aging in the SIRT6 knockout mouse. SIRT6-deficient mice, as well as several mouse models of nucleotide excision repair deficiency, exhibit a premature aging phenotype, which is associated with insulin signaling (16). This premature aging phenotype in mice is associated with dysregulation of insulin signaling as a result of glucose metabolism dysfunction (16,20), hyperactive NF-κB signaling (17), and genomic instability (7). SIRT6 is involved in all these pathways. With regard to humans, mesenchymal stem cells deficient in SIRT6 have dysregulated redox metabolism because SIRT6 functions as a transactivator for nuclear factor erythroid 2-related factor 2, establishing a connection between SIRT6 and oxidative stress (21). The imbalanced relationship between DNA repair and metabolism in SIRT6-deficient mice is an important theme in premature aging. The upregulation of NF-κB as a consequence of SIRT6 deficiency further illustrates the multiple connections of SIRT6 with premature aging. We sought to investigate the importance of DNA repair and NF-κB in a tissue culture model. We explored the effects of SIRT6 knockdown in human dermal fibroblasts under normal conditions and after environmental stress from ultraviolet B (UVB) and ultraviolet A (UVA) irradiation. In this report, we evaluated the effectiveness of

SIRT6 as a protective molecule in relation to the extent of DNA damage and the level of NF-κB expressed under normal conditions and after UV exposure of normal human dermal fibroblasts.

MATERIALS AND METHODS

TISSUE CULTURE

Neonatal human dermal fibroblasts were purchased from Life Technologies. Cells were maintained in Dulbecco Modified Eagle's Media (DMEM; Life Technologies, Grand Island, NY) and 10% fetal bovine serum (FBS) (HyClone, GE Heathcare, Logan, UT). Cells were grown at 37ºC and 5% humidity. Donor 828840 was used at p5 and at p8 for the SIRT6 electroporation, comparing SIRT6 messenger RNA (mRNA) levels relative to RPLPO mRNA levels. Donor 871299 was used for the NF-κB experiment at passage 5. Donor 904886 was used for the first comet assay, 40 mJ/cm^2 UVB and 5, 10, or 20 J/m^2 UVA, at passage 12. Donor 871299 was used for the second comet assay, 40 mJ/cm^2 UVB and 20 J/m^2 UVA, at passage 6.

ELECTROPORATION OF SMALL-INTERFERING RNA

The Amaxa Nucleofector II/2b Lonza Electroporation Kit (Cologne, Germany) was used to deliver small-interfering RNA (siRNA) specific for SIRT6. Cells were washed with Hank's buffered saline solution before trypsinizing. An optimized electroporation protocol, ID 83, from Lonza was followed. The fibroblast pellet was resuspended in the appropriate buffer and supplement (Lonza electroporation kit, VPD-1001). The Nucleofector II/2b was set to program U-020. Silencing was achieved using an ON-TARGETplus SMARTpool for SIRT6 from Dharmacon (Lafayette, CO) containing the following sequences: 5′-CCAAGUGUAAGACGCAGUA-3′, 5′-GUACAUCGCUGCAGAUCCG-3′, 5′-CCAAAAGGGUGAAGGCCAA-3′, and 5′-GAACUGGCGAGGCUGGUCU-5′ or the single sequence synthesized from Dharmacon, 5′-GGAACAUGUUUGUGGAAGAUU-3′ (22). The ON-TARGETplus nontargeting (NT) pool from Dharmacon included the four following sequences: 5′-UGGUUUACAUGUCGACUAA-3′, 5′-UGGUUUACAUGUUGUGUGA-3′, 5′-UGGUUUACAUGUUUUCUGA-3′, and 5′-UGGUUUACAUGUUUUCCUA-3′. Each electroporation included 8–10 × 10^5 fibroblasts. Prior to electroporation, each cell pellet was resuspended by adding a volume of 105 μl of Lonza buffer containing siRNA at a final concentration of 1 μM. The resuspended pellet was transferred to a cuvette for electroporation. Electroporated fibroblasts were seeded in four wells of a six-well plate or a 100-mm plate and incubated in 10% FBS and DMEM.

RNA PURIFICATION AND REAL-TIME REVERSE TRANSCRIPTION POLYMERASE CHAIN REACTION

Neonatal fibroblasts were washed with Dulbecco's phosphate-buffered saline (DPBS) prior to extracting with 600 μl of RLT buffer from the RNeasy mini kit (Qiagen, Hilden,

Germany). The RNA extract was applied to a QIAshredder column (Qiagen) and eluted. The extract was further purified according to the RNeasy protocol. The RNA concentration was determined by absorbance at 260 nm with a Beckmann DU-7000 (Brea, CA) spectrophotometer (1A = 40 μg/ml). RNA was reverse transcribed with a high-capacity complementary DNA reverse transcription kit (Applied Biosystems, Foster City, CA) and amplified with Taqman primer/probe sets from Applied Biosystems specific for human SIRT6, assay ID Hs00966001_m1, and RPLPO (60S acidic ribosomal protein P0), assay ID Hs00420895_gH. Real-time reverse transcription polymerase chain reaction (PCR) was performed and analyzed on an Applied Biosystems 7500 Fast instrument. Each PCR cycle involved 3 s at 95°C for melting and 60 s at 60°C for annealing and extension. A total of 40 cycles were completed.

MODULATION OF NF-KB

Neonatal fibroblasts were electroporated with SIRT6 siRNA and incubated for 48 h (21) before exposing the cells to 40 or 80 mJ/cm^2 UVB. These doses were not cytotoxic to neonatal fibroblasts (data not shown). An irradiation chamber, BS-03 (manufactured by Dr. Grőbel UV-Elektronik GmbH, Ettlingen, Germany), was used to deliver the UVB. Six hours after irradiation, the cells were lysed and the total protein was extracted with NE-PER nuclear and cytoplasmic extraction kit from Thermo Fisher Scientific (Waltham, MA). Total protein was quantitated with a Micro BCA protein assay kit from Thermo Fisher Scientific. A chemiluminescent transcription factor detection kit from Thermo Fisher Scientific was used to detect NF-κB p50. A Molecular Devices SpectraMax M2e (Sunnyvale, CA) was used to measure chemiluminescence.

DETECTION OF DNA DAMAGE

Each well of a Trevigen comet slide (Gaithersburg, MD) was seeded with 10,000 electroporated fibroblasts in 200 μl of DMEM and 10% FBS. The neonatal fibroblasts were previously electroporated with SIRT6 siRNA or NT siRNA (NT). After 48 h of growth, neonatal fibroblasts were exposed to 40 mJ/cm^2 UVB and 20 J/cm^2 UVA using the BS-03 irradiation chamber. Cells were exposed to UV at room temperature. Cells were grown for another 4 h at 37°C and 5% humidity before processing the slides with Trevigen reagents. No inhibitors of DNA repair were added. Slides were washed with DPBS and 75 μl of melted agarose was pipetted on each well. The cells were then processed according to the Trevigen protocol with the following changes. After 10 min at 4°C, cells were lysed for 3 h on ice. Slides were removed from the lysis solution and placed into the alkaline solution for 30 min. Slides were electrophoresed in a cold alkaline solution (300 mM NaOH, 1 mM ethylenediaminetetraacetic acid, pH > 13) for 30 min at 23 V. After electrophoresis, slides were rinsed with water, fixed with 70% ethanol for 5 min, and dried overnight. DNA was detected with 50 μl SYBR Green (Thermo Fisher) per well (diluted 1:10,000 in TE buffer) and incubated for 5 min at 4°C. Slides were viewed under an Olympus BX51 microscope (Center Valley, PA) using a Fluorescein Isothiocyanate filter and a 20× objective. Images were captured using Nikon Elements Software (Melville, NY). The tail moments were determined with Comet Score software from TriTek (Wilmington, DE).

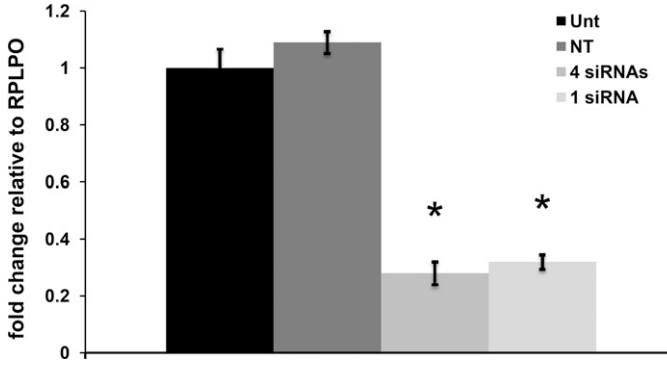

Figure 1. Neonatal fibroblasts were electroporated using four siRNAs specific for SIRT6 or a single siRNA for SIRT6 (22). An average of 70% knockdown was observed after 48 h relative to the nontargeted cells from three separate experiments. Data are expressed as mean ± SEM, $*p < 0.005$.

RESULTS

SIRT6 KNOCKDOWN

Neonatal human dermal fibroblasts were electroporated with SIRT6 siRNA and the mRNA levels for SIRT6 were monitored 48 h after electroporation. A 72% decrease in SIRT6 mRNA was achieved with four siRNAs and a 68% decrease with one SIRT6 siRNA (Figure 1). The NT siRNA level of SIRT6 mRNA was comparable to the untreated.

IMPACT OF SIRT6 KNOCKDOWN ON NF-κB

SIRT6 knockdown elevates NF-κB p50 levels significantly in the absence of UVB (Figure 2). NF-κB p50 levels were monitored 52 h after electroporation using an enzyme-linked

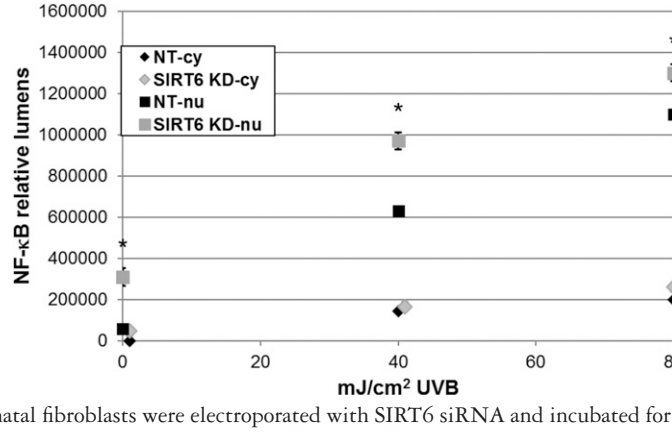

Figure 2. Neonatal fibroblasts were electroporated with SIRT6 siRNA and incubated for 48 h before exposing to UVB. Six hours later, cells were lysed. The nuclear fraction (squares) was separated from the cytosolic faction (diamonds) and probed for NF-κB p50 (NT-cy, -nu = non-targeting cytosolic or nuclear; SIRT6 KD-cy, -nu = SIRT6 knockdown cytosolic or nuclear). In the absence of UVB, SIRT6 knockdown increased NF-κB translocation to the nucleus fourfold relative to NT. Data expressed as mean ± SEM, $*p < 0.05$.

immunosorbent assay antibody detection assay. A 4.3-fold increase in chemiluminescence was observed in cells receiving SIRT6 siRNA relative to NT siRNA. A transient reduction in SIRT6 mRNA levels was sufficient to elevate NF-κB p50 levels more than fourfold relative to the NT cells.

In the presence of UVB, the SIRT6 knockdown fibroblasts continued to generate more chemiluminescence relative to the NT fibroblasts, but the differential decreased as the UV dose increased (Figure 2). Exposure of the SIRT6 knockdown cells to 40 or 80 mJ/cm^2 of UVB increased NF-κB p50 levels about fivefold and sixfold, respectively, to SIRT6 knockdown cells not receiving UVB. However, the differential between the SIRT6 knockdown cells and the NT cells after receiving 40 mJ/cm^2 was about 1.5-fold and after receiving 80 mJ/cm^2, the differential was 20%. Cytosolic levels of NF-κB p50 remained low in the presence or absence of UVB. Thus, the largest differential increase in NF-κB levels of the SIRT6 knockdown cells versus the NT fibroblasts occurred without UV exposure. The addition of UV increased nuclear NF-κB levels for both the NT and the SIRT6 knockdown, but the differential decreased as the dose of UV increased.

IMPACT OF SIRT6 KNOCKDOWN ON DNA DAMAGE

In the absence of UV, SIRT6 knockdown increases the tail moment about 10-fold relative to the NT fibroblasts (Figure 3). Cells were lysed 4 h after UV exposure. Examination of nuclear DNA by fluorescent microscopy with SYBR Green staining revealed a circular shape for the NT fibroblasts and the SIRT6 KD cells, reflecting a compact nucleus (Figure 4). In the absence of UV, SIRT6 KD cells had a visible tail.

After UV, SIRT6 knockdown cells increased their tail moment about twofold relative to the NT fibroblasts (Figure 3). Cells were allowed 4 h to repair the DNA damage resulting from 40 mJ/cm^2 UVB and 20 J/cm^2 UVA. The nucleus appeared fractured for the NT fibroblasts and the SIRT6 KD cells with a visible comet tail (Figure 4).

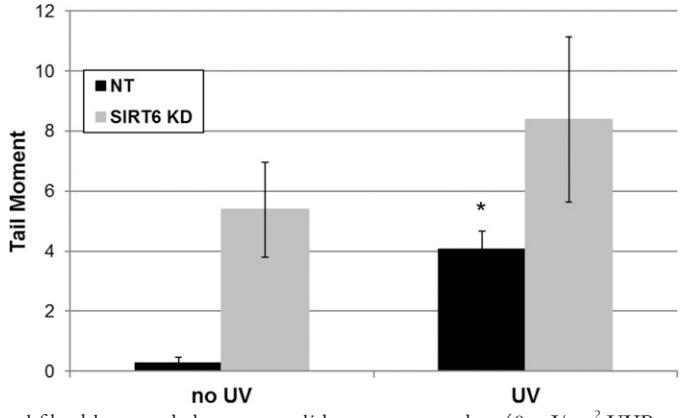

Figure 3. Neonatal fibroblasts seeded on comet slides were exposed to 40 mJ/cm^2 UVB and 20 J/cm^2 UVA. Cells were grown for another 4 h before processing the slides. SIRT6 knockdown increased the tail moment about fivefold relative to the nontargeted, whereas no significant change was observed when UV was added. Data are expressed as mean ± SEM, *$p < 0.05$.

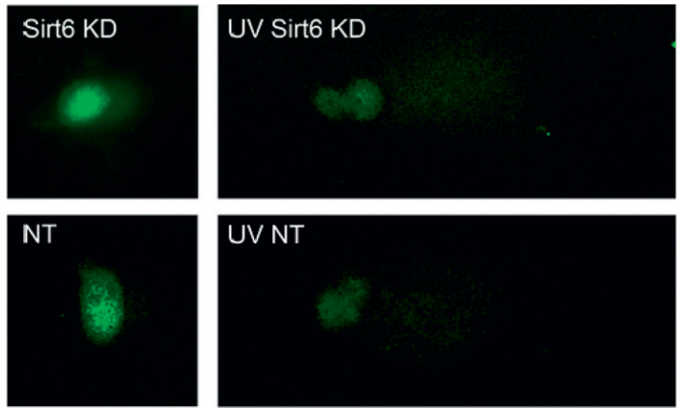

Figure 4. Four hours after UV, cells were lysed with an alkaline solution and electrophoresed. DNA was detected with SYBR Green and viewed at 200×.

DISCUSSION

The physical interaction between SIRT6 and the NF-κB subunit, RelA, is required for the deacetylation of histones associated with NF-κB target gene promoters. Loss of suppression of this proinflammatory pathway results in a shortened lifespan for the mouse (17). The increase in NF-κB levels we measured are in agreement with this finding as well as data reported for human fibroblasts transfected with SIRT6 siRNA and Lipofectamine (22). However, we did not observe a change in COL1 mRNA levels 48 h after electroporation as reported by Baohau and Li, despite using the same siRNA sequence (data not shown). The discrepancy might be explained by the delivery method employed. Nevertheless, we did observe a strong increase in p50, about 4.3-fold, 52 h after SIRT6 knockdown relative to the NT cells. The addition of UVB to cells electroporated with SIRT6 siRNA or NT siRNA increased nuclear NF-κB levels further for both electroporated populations; however, the differential decreased as the dose of UVB increased. The reported physical interaction of SIRT6 with the NF-κB subunit, RelA, and corepressor function of SIRT6 achieved by silencing NF-κB target genes through deacetylation of H3K9 at target gene promoters helps to explain our observations (17).

Mammalian cells deficient in SIRT6 are, as a consequence, defective in several capacities for DNA repair including BER (6–8), DSB repair (7,9–12), and telomere maintenance (7,13,14). A fivefold increase in the tail moment was measured with SIRT6 KD fibroblasts relative to NT fibroblast. We interpret this result as a decrease in endogenous DNA repair capacity resulting from a change in SIRT6 activity and/or SIRT6 protein levels. The increase observed in the tail moment for the knockdown cells might result from single strand breaks not repaired during G_1 phase of the cell cycle and becoming DSBs during S-phase (23). Exposure of SIRT6 KD fibroblasts to UV increased the tail moment about twofold relative to NT fibroblasts exposed to the same dose of UV. The addition of UVA will initiate more free radicals associated with DNA damages, which are not repaired. These data support the role of SIRT6 in maintaining genome integrity.

Transient knockdown of SIRT6 mRNA was sufficient to impact genomic stability as reflected in the tail moment of SIRT6 KD cells without UV as well as the upregulation of NF-κB in the absence of UVB. These SIRT6 functions were not compensated for by other cellular

pathways during transient knockdown. A compensatory metabolic response previously reported would include an increase in glycolysis and more glucose uptake (24). Likewise, an increase in DNA damage leads to an increase in NF-κB activation. The concomitant increase in NF-κB signaling can result in a feed-forward loop of more cellular stress and additional DNA damage. In this model, we were able to show that SIRT6 plays a critical role in reducing skin inflammation and initiating DNA repair. In conclusion, our results demonstrate the importance of SIRT6 in maintaining genomic integrity and controlling inflammation, both of which are essential for maintaining a young and healthy skin.

Taken together, our data provide a link between sirtuin activity, which has received much attention due to its association with gene silencing and its potential for increasing cell longevity, and two parameters of cellular health: NF-κB and DNA damage. Since increased NF-κB translocation leads to higher levels of inflammation and increased DNA damage contributes to apoptotic cell formation, both of which generate reactive oxygen species, attenuation of these effects by maintaining SIRT6 activity in the nucleus will protect skin cells against the kinds of damage that can over time develop into fine lines and wrinkles. Finding new biological materials that will achieve this goal is an important next step.

REFERENCES

(1) M. Serravallo, J. Jagdeo, S. A. Glick, D. M. Siegel, and N. I. Brody, Sirtuins in dermatology: Applications for future research and therapeutics, *Arch. Dermatol. Res.,* **305,** 269–282 (2013).
(2) E. Pelle and N. Pernodet, "Sirtuins: Biology and Anti-aging Benefits for Skin Care," in *Harry's Cosmetology, 9th Ed*, M. Rosen Ed. (Chemical Publishing, Los Angeles, CA, 2015), pp. 1177–1189.
(3) S. Kugel and R. Mostoslavsky, Chromatin and beyond: The multitasking roles of SIRT6, *Trends Biochem. Sci.,* **39,** 72–81 (2014).
(4) L. Bosch-Presegué and A. Vaquero, Sirtuins in stress response: Guardians of the genome, *Oncogene,* **33,** 3764–3775 (2014).
(5) T. L. A. Kawahara, N. A. Rapicavoli, A. R. Wu, K. Qu, S. R. Quake, and H. Y. Chang, Dynamic chromatin localization of SIRT6 shapes stress- and aging-related transcriptional networks, *PLoS Genet.,* **7,** e1002153 (2011).
(6) R. Mostoslavsky, K. F. Chua, D. B. Lombard, W. W. Pang, M. R. Fischer, L. Gellon, P. Liu, G. Mostoslavsky, S. Franco, M. M. Murphy, K. D. Mills, P. Patel, J. T. Hsu, A. L. Hong, E. Ford, H.-L. Cheng, C. Kennedy, N. Nunez, R. Bronson, D. Frendewey, W. Auerbach, D. Valenzuela, M. Karow, M. O. Hottiger, S. Hursting, H. C. Barrett, L. Guarente, R. Mulligan, B. Demple, G. D. Yancopoulos, and F. W. Alt, Genomic instability and aging-like phenotype in the absence of mammalian SIRT6, *Cell,* **124,** 315–329 (2006).
(7) R. I. Tennen and K. F. Chua, Chromatin regulation and genome maintenance by mammalian SIRT6, *Trends Biochem. Sci.,* **36,** 39–46 (2011).
(8) D. B. Lombard, Sirtuins at the breaking point: SIRT6 in DNA repair, *Aging,* **1,** 12–16 (2009).
(9) Z. Mao, C. Hine, X. Tian, M. van Meter, M. Au, A. Vaidya, A. Seluanov, and V. Gorbunova, SIRT6 promotes DNA repair under stress by activating PARP1, *Science,* **332,** 1442–1446 (2011).
(10) A. Kaidi, B. T. Weinert, C. Choudhary, and S. P. Jackson, Human SIRT6 promotes DNA-end resection through CtIP deacetylation, *Science,* **329,** 1348–1353 (2010).
(11) T. L. A. Kawahara, E. Michishita, A. S. Adler, M. Damian, E. Berber, M. Lin, R. A. McCord, K. C. L. Ongaigui, L. D. Boxer, H. Y. Chang, and K. F. Chua, SIRT6 recruits SNF2H to DNA break sites, preventing genomic instability through chromatin remodeling, *Mol. Cell,* **51,** 454–468 (2013).
(12) Z. Mao, X. Tian, M. Van Meter, Z. Ke, V. Gorbunova, and A. Seluanov, Sirtuin 6 (SIRT6) rescues the decline of homologuous recombination repair during replicative senescence, *Proc. Natl. Acad Sci USA,* **109,**11800–11805 (2012).
(13) G. Jia, L. Su, S. Singhal, and X. Liu, Emerging roles of SIRT6 on telomere maintenance, DNA repair, metabolism and mammalian aging, *Mol. Cell Biochem.,* **364,** 345–350 (2012).
(14) E. Michishita, R. A. McCord, E. Berber, M. Kioi, H. Padilla-Nash, M. Damian, P. Cheung, R. Kusumoto, T. L. A. Kawahara, J. C. Barrett, H. Y. Chang, V. A. Bohr, T. Ried, O. Gozani, and K. F. Chua, SIRT6 is a histone H3 lysine 9 deacetylase that modulates telomeric chromatin, *Nature,* **452,** 492–496 (2008).

(15) R. D. Ley, Photorepair of pyrimidine dimers in the epidermis of the marsupial *Monodelphis domestica*, *Photochem. Photobiol.,* **40,** 141–143 (1984).
(16) J.-P. Etchegaray, L. Zhong, and R. Mostoslavsky, The histone deacetylase SIRT6: At the crossroads between epigenetics, metabolism and disease, *Curr. Top. Med. Chem.,* **13,** 2991–3000 (2013).
(17) T. L. A. Kawahara, E. Michishita, A. S. Adler, M. Damian, E. Berber, M. Lin, R. A. McCord, K. C. L. Ongaigul, L. D. Boxer, H. Y. Chang, and K. F. Chua, SIRT6 links histone H3 lysine 9 deacetylation to NF-κB-dependent gene expression and organismal life span, *Cell,* **136,** 62–74 (2009).
(18) G. Natoli, When sirtuins and NF-κB collide, *Cell,* **136,** 19–21 (2009).
(19) Y. Kanfi, S. Naiman, G. Amir, Y. Peshi, G. Zinman, L. Nahum, Z. Bar-Joseph, and H. Y. Cohen, The sirtuin SIRT6 regulates lifespan in male mice, *Nature,* **483,** 218–221 (2012).
(20) R. Mostoslavsky, DNA repair, insulin signaling and sirtuins: At the crossroads between cancer and aging, *Front. Biosci.,* **13,** 6966–6990 (2008).
(21) H. Pan, D. Guan, X. Liu, J. Li, L. Wang, J. Wu, J. Zhou, W. Zhang, R. Ren, W. Zhang, Y. Li, J. Yang, Y. Hao, T. Yuan, G. Yuan, H. Wang, Z. Ju, Z. Mao, J. Li, J. Qu, F. Tang, and G.-H. Liu, SIRT6 safeguards human mesenchymal stem cells from oxidative stress by coactivating NRF2, *Cell Res.,* **26,** 190–205 (2016).
(22) Y. Baohua and L. Li, Effects of SIRT6 silencing on collagen metabolism in human dermal fibroblasts, *Cell Biol. Int.,* **36,** 105–108 (2012).
(23) K. Wischermann, S. Popp, S. Moshir, K. Scharffetter-Kochanek, M. Wlaschek, F. de Gruijl, W. Hartschuh, R. Greinert, B. Volkmer, A. Faust, A. Rapp, P. Schmezer, and P. Boukamp, UVA radiation causes DNA strand breaks, chromosomal aberrrations and tumorigenic transformation in HaCaT skin keratinocytes, *Oncogene,* **27,** 4269–4280 (2008).
(24) L. Zhong, A. D'Urso, D. Toiber, C. Sebastian, R. E. Henry, D. D. Vadysirisack, A. Guimaraes, B. Marinelli, J. D. Wikstrom, T. Nir, C. B. Clish, B. Vaitheesvaran, O. Iliopoulos, I. Kurland, Y. Dor, R. Weissleder, O. S. Shirihai, L. W. Ellisen, J. M. Espinosa, and R. Mostoslavsky, The histone deacetylase Sirt6 regulates glucose homeostasis via HIF-1α, *Cell,* **140,** 280–293 (2012).